Structure and Properties of an Exceptional Low Molecular Weight Hydrogelator

Arno M. Bieser and Joerg C. Tiller*

Freiburger Materialforschungszentrum, Albert-Ludwigs-Universität Freiburg, Stefan-Meier-Strasse 21, 79104 Freiburg, Germany

Received: June 26, 2007; In Final Form: August 17, 2007

Research for low molecular weight (LMW) hydrogelators has become an area of increasing interest due to many possible new applications for such compounds. They might serve as templates for nanostructures or in biomedical applications and even in drug discovery. In this investigation, we explored the structure-gelling relations of a LMW hydrogelator that can form a hydrogel in water at room temperature. To this end, various analytical techniques such as nuclear magnetic resonance, rheology, X-ray scattering, birefringence, and microscopy were applied to gain better insight on the structure of the gel and to provide an explanation for this unique gelation behavior.

Introduction

Gels represent a unique class of soft matter consisting of three-dimensional networks that immobilize a liquid component in a continuous structure of macroscopic dimensions.[1] Depending on the type of liquid component, gelators can be classified into organogelators and hydrogelators. The latter ones are of particular interest since they play an important role in nature as well as in everyday life. They are known from their use in cosmetics such as hair gel as well as in familiar foods such as jelly or pudding. Moreover, they are also intriguing materials for medical applications[2] as well as for analytical,[3] environmental,[4] and material science.[5]

Another important distinction concerning gelators has to be made depending on the type of interactions between the aggregating molecules. In chemical gels, the entire solid phase is kept together through covalent bonds. Therefore, polymer hydrogels typically possess elastic properties similar to solid materials and—like in the case of cross-linked polymers—the networks can be swollen or shrunk by the addition or removal of solvent. Because of the covalent nature of the bonds, formation of these gels is irreversible. In contrast, physical gels are composed of supramolecular assemblies of low molecular weight (LMW) molecules held together by physical interactions such as hydrophobic associations and van der Waals forces,[6] hydrogen bonding,[7] ionic bonding,[8] and combinations of these forces.[9] This results in less robust systems with weaker mechanical resistance as compared to polymer hydrogels. Such LMW hydrogelators enjoyed little practical use, and although already known for over 100 years,[10] little attention was paid to their development. Furthermore, only a few publications reported on the systematic structure elucidation of such systems. One of the few examples is an exceedingly detailed and comprehensive study of Menger and Caran in which the authors highlight the challenges and difficulties in such an approach and the necessity of applying manifold analytical techniques to obtain insight on the architecture of gels of LMW gelators.[11]

In recent years, it was found that LMW gelators exhibit some interesting properties.[12,13] The non-covalent nature of their bonds often leads to thermally reversible but highly ordered structures. Like similar supramolecular aggregates, such gels can possibly self-replicate and thereby possess the feature of built-in error correction. This means that if the highly ordered structure of the gel is destroyed (e.g., by a mechanical influence such as stirring), the molecules afterward can move and rearrange themselves to reestablish the gel structure with its higher ordering.[14] Thus, they have exceptional promise, for example, as smart materials in the design of scaffolds.[15] Another field of great interest is biomedical applications. Since LMW hydrogels are composed of small molecules, they are usually easier to degrade by organisms and could serve as vesicles for controlled drug release where biocompatibility and biodegradability are an important prerequisite.[16] Even more intriguing are new possibilities that might arise from hydrogelators that possess biological activity themselves.[17] Xing et al. reported on a hydrogelling antibiotic that exhibits a manifold higher activity than the comparable but non-hydrogelling analogue due to local concentration on the bacterial cell surface.[18] We could scrutinize this new concept with the aid of a novel LMW hydrogelator (1-(2-*n*-hexylphenylazo)-2-hydroxy-6-naphthalenesulphonate, OHD) as the model compound. OHD is capable of gelling selectively on cationic surfaces far below its critical gelation concentration (MGC).[19]

It turns out that the hydrogel prepared from this gelator is quite uncommon (i.e., it consists of highly ordered and stable hierarchic structures, which can be preserved upon freeze-drying). This resulted in the first solid LMW hydrogelator that formed a hydrogel in water without heating. Here, we present a detailed investigation on the inner structure of the hydrogel and the gelling mechanism of this unusual hydrogelator.

Materials and Methods

Synthesis of OHD. A detailed procedure for the synthesis and purification as well as analytical data of OHD is provided in ref 19.

Preparation of Hydrogels. In a typical procedure, the required quantity of OHD was mixed with 5−10 mL of water in a test tube (20 mL). The resulting mixture was heated to 80 °C to afford a clear homogeneous solution that on cooling to ambient temperature produced the hydrogel.

* Corresponding author. Fax: (+49) 761 203 4700; e-mail: joerg.tiller@fmf.uni-freiburg.de.

10.1021/jp074953w CCC: $37.00
Published on Web 11/01/2007

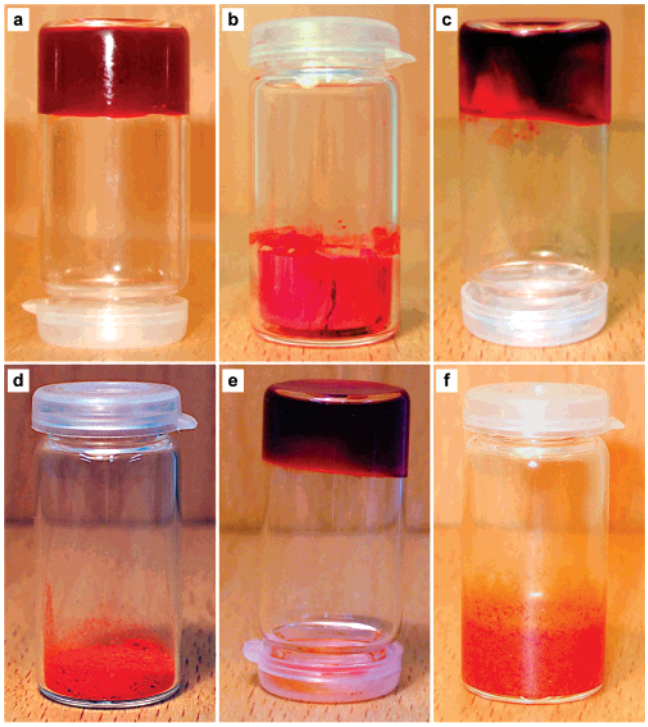

Figure 1. (a) Original hydrogel of 5 wt % of OHD in water. (b) Xerogel of the freeze-dried hydrogel of OHD. (c) Rehydrogelled xerogel 48 h after wetting the freeze-dried sample of the xerogel with the previously evaporated volume of water. (d) Ground xerogel before wetting with water. (e) Gelled sample of the ground xerogel. (f) 5 wt % crystalline OHD in water at room temperature showing that no hydrogel forms without heating.

Preparation of Xerogels. The tube with the hydrogel was immersed in liquid nitrogen until the sample was completely frozen. The frozen sample was dried in vacuo for 24 h.

Preparation of Crystals and Needles. Crystalline assemblies were formed by slow evaporation of water from a test tube containing a sample of the hydrogel of OHD of 5 wt %.

Gelling Test. Gelation was considered to have occurred when the solid aggregate mass was stable to inversion when the sample bottle was turned upside down.[20]

NMR. NMR spectra were recorded in D_2O in a Bruker ARX 300 spectrometer operating at 300 MHz. Chemical shifts are reported relative to residual non-deuterated solvent.

Polarizing Optical Light Microscopy (POM). POM was performed on a Leitz-Ortholux II Poll-BK microscope using a Mettler FP80/82 thermally controlled stage. For cooling, a nitrogen flow cooled by liquid nitrogen was channeled around the sample. The following occurred in the preparation of samples for POM measurements: for the investigation of the crystals, a small needle was placed on a microscope slide, and a drop of water was put on top of it. For the measurements of the hydrogels, a small quantity of gel was put on a microscope slide. The sample was covered with a glass coverslip, which was sealed immediately at the edges with glue to prevent the evaporation of water. For the determination of the phase transition temperatures and temperature dependence of the phases, heating and cooling rates of 2 K/min were applied. Gel melting points were determined by the disappearance of birefringence between crossed polars.

Other Microscopy. Visible microscopy images were taken with an Axioplan 2 imaging microscope (Zeiss). The electron microscope images were measured with a field emission scanning electron microscope LEO 1525 after previous sputtering with gold/palladium in a Polaron Sputter Coater SC 7640.

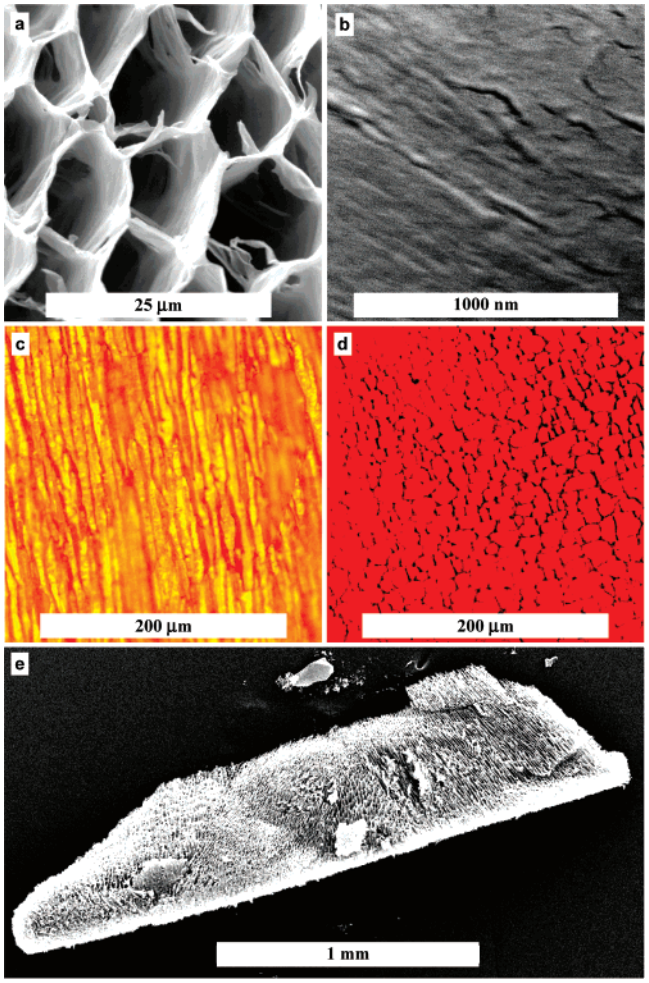

Figure 2. (a) SEM image showing the channel structuring of a xerogel of OHD. (b) SEM image of fibers in a xerogel of OHD. (c and d) Channels of xerogels of OHD examined by light microscopy. (e) ESEM image of a larger xerogel fragment.

Rheological Characterization. Rheological measurements were carried out on a stress-controlled mechanical spectrometer UDS200 (Paar Physica) with parallel plate geometry. The radius of the plates was 50 mm. A Peltier device controlled the temperature of the bottom plate. In a typical experiment, a volume of 2.0 mL of gel was distributed on the ground plate of the rheometer. Then, the top plate was lowered until the resulting film of the gel was spread evenly between the plates leading to a gap of approximately 0.9−1.1 mm. The edges of the two plates were sealed with a subtle layer of low viscosity oil, inhibiting evaporation of water and composition changes of the sample during the measurements. Furthermore, the instrument was fitted with an environmental chamber, which allowed us to maintain an atmosphere saturated with water.

X-ray Measurements. The X-ray data were collected at room temperature using a Ni-filtered Cu− Kα beam ($\lambda = 1.54$ Å) collimated by a 0.8 mm collimator. The scattered X-ray intensity was detected by an image plate system (700 pixels × 700 pixels, 250 mm resolution). The samples were measured in 2 mm glass tubes. The following occurred in the preparation of samples for X-ray measurements. Hydrogels: to ensure highly ordered and representative structures without disturbances due to shearing and stress, samples of the hydrogels were prepared as follows: solutions of OHD were prepared by dissolving the appropriate amount of OHD in distilled water at 80 °C. Next, the solutions were put into a glass syringe warmed to 80 °C, and the solutions were inserted into the bottom of an accordingly preheated glass

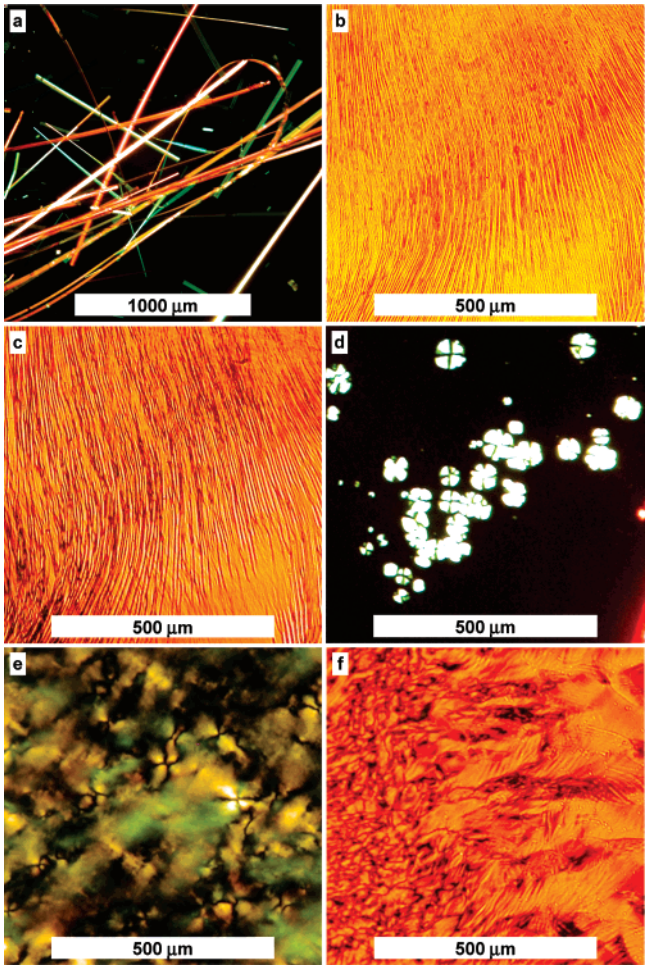

Figure 3. (a) Polarizing microscopy image of virgin crystals of OHD. (b) Optical textures examined under non-polarized light shown by a hydrogel of 5 wt % OHD in water formed during cooling from the isotropic solution. (c) Same domain as in panel b seen with crossed polars. (d) Focal conic domains of the hydrogel before tempering. (e) Texture observed at room temperature at the original hydrogel before tempering. (f) Schlieren and fan-like textures of OHD after tempering.

capillary via a needle. The capillary was then allowed to cool slowly to room temperature, and thus, the gel formed. The top of the tube was sealed with a vacuum crease, which acted as a moisture barrier. Xerogels: samples of the xerogels were carefully inserted into the glass capillaries and measured without further manipulation.

Molecular Modeling. Semiempirical calculations were carried out using the CAChe program (version 6.1.12), which was provided by Fujitsu.

Results and Discussion

Gelation Experiments. All hydrogels formed from solid LMW hydrogelators in water were prepared by heating the sample and cooling it to room temperature or by ultrasonication[21−24] or both.[8,25,26] This is also the case for OHD, which has to be heated to 80 °C prior to forming a hydrogel at room temperature. However, the formed gel was found to be exceptionally stable over weeks (cf. Figure 1a). More interestingly, we found that the solid obtained by lyophilization did form a hydrogel without heating the sample (Figure 1b,c). Even grinding the solid did not diminish its properties of hydrogelling without heating. Under microscopic investigations, the xerogels of such gels showed the same ordering such as the ones obtained from gels formed by heating. Such a capacity is usually only found with

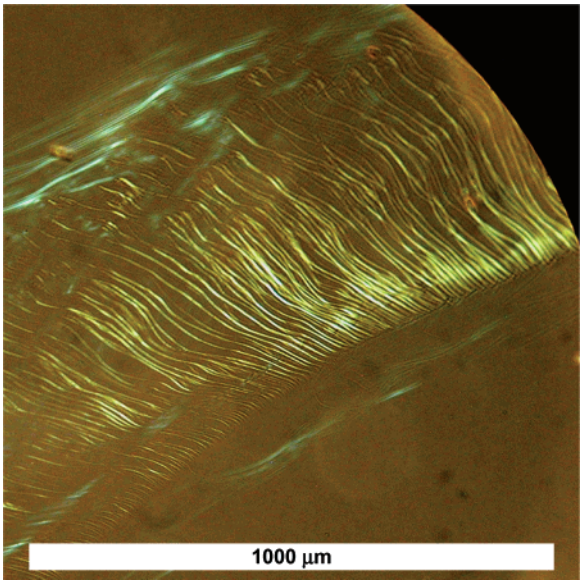

Figure 4. Polarizing microscopy image of a diluted sample of OHD of 2 wt % with the initial structuring spreading out.

TABLE 1: Concentration Dependence of the Phase Transition Temperatures in Hydrogels of OHD with GS Meaning Gel to Solution and SG Meaning Solution to Gel

concn (wt %)	T_{GS} (°C)	T_{SG} (°C)
4	48.6	42.7
5	50.6	46.7
6	53.2	47.8

macromolecular gelators, where gel formation is mainly driven by the increase of entropy in the course of swelling of polymeric matrices.

From this, we presume that OHD must form a very stable polymer-like structure in the gel. In our previous studies, we have examined such hydrogels and also freeze-dried samples with the help of AFM, environmental scanning electron microscopy, and light microscopy. It was found that the structures of the wet gels and of the xerogels are comparable and composed of a highly ordered honeycomb-like arrangement of channels or tubes of several micrometers in diameter that are oriented in parallel (Figure 2 a and ref 19 Figure 2b−e). Figure 2a,d shows top views of the channels. As can be seen, the arrangement exhibits a rather high regularity concerning the size and distribution of the channels. This regularity is also found throughout large domains of several millimeters in length as can be seen in Figure 2e. In the wet state, these tubes contain water, whereas they are empty in the xerogels. However, this structure cannot explain the hydrogelling of the xerogel powder because grinding has destroyed the structures of dimensions in the micrometer range, and still hydrogelation occurs without heating. Therefore, the microscopic arrangement within the walls of the honeycombs must be responsible for the hydrogelling. To detect the nature of this ordering, we performed high-resolution SEM investigations of xerogels. We found fibers with dimensions approximately between 10 and 20 nm as shown in Figure 2b. These fibers seem to form the walls of the channels of Figure 2a.

POM. Amphiphilic molecules such as OHD are known to show different kinds of ordering. Less ordered micelles are usually the dominating form of aggregation at low concentrations or at higher temperatures. Progressive ordering of the system takes place at higher concentrations or at lower temperatures. This often leads to phases with long-range transla-

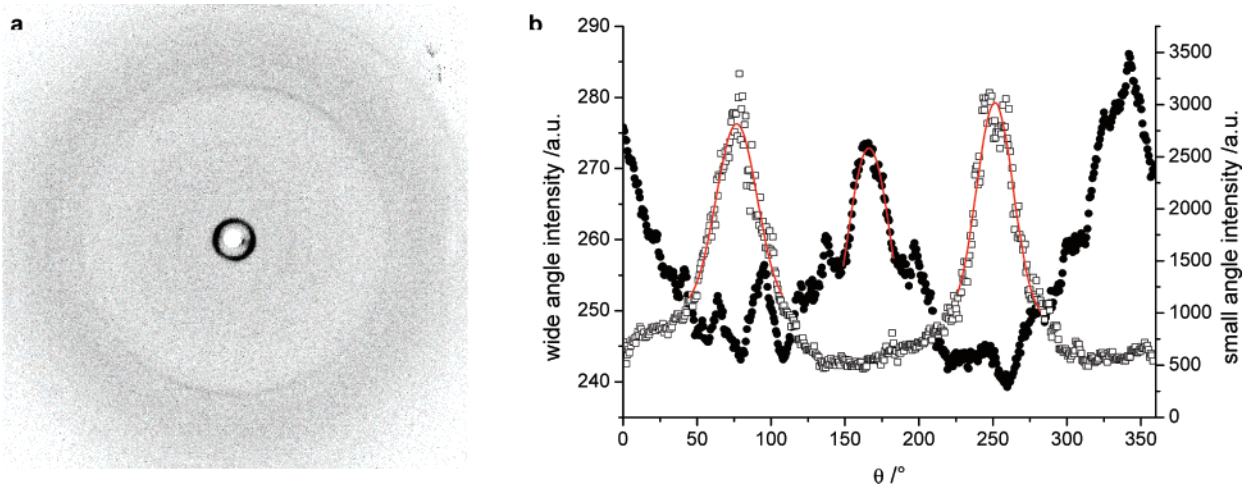

Figure 5. (a) X-ray diffraction pattern of a xerogel obtained from a hydrogel of 6 wt %. (b) Azimuthal intensity profiles presenting wide angle reflection (●) and small angle reflection (□). Solid lines represent the curves fitted using the Gaussian distribution. The small angle reflection corresponds to a layer spacing of 40 Å.

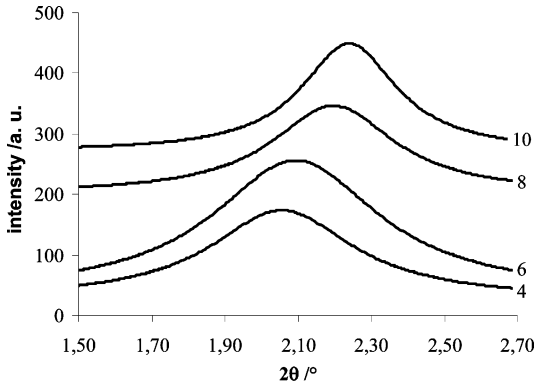

Figure 6. X-ray investigation of xerogels obtained from hydrogels with different concentrations. The lines represent the curves fitting the data to a Lorentzian function. The numbers on the right give the concentrations of the gel in wt %.

tional ordering.[27] Under suitable conditions of temperature, pressure, and concentration, such systems can exist as a mesophase. With its two disc-like aromatic moieties and the azo group as the linking unit, OHD possess all the prerequisites of a mesogen, and so we characterized the liquid crystalline behavior by POM.

Samples of crystals of OHD as well as hydrogels showed birefringence (Figure 3). Mesophases could be found at minimum concentrations of about 2 wt %. Addition of water to crystals as well as to aqueous gels caused dilution of the samples until only limited areas of birefringence were visible. Further dilution led to the complete disappearance of birefringence. Typical textures of the gels were identified by comparison of the observed mesophases with textures described in the literature.[28−30] Focal conic domains (Figure 3d) were indicative for the presence of bilayers or lamellar phases. Such phases are comparable to the smectic A phases of thermotropic liquid crystals. Further characteristic textures for these phases are the schlieren textures as can be seen in Figure 3e,f. These textures are also observed frequently for other liquid crystalline azo compounds.[31−34] Remarkable structural changes take place during the thermal cycling of the gels. Lyotropic hexagonal phases are formed spontaneously and quickly after heating the gel and cooling the isotropic solution (Figure 3b,c). Obviously, this hexagonal packing leads to assemblies, which are oriented in parallel and are hundreds of micrometers in length. The structures also can be seen without a polarizer (Figure 3b).

Once formed, the structures seem to represent the final ordering of OHD, except that for minor domains with schlieren and fan-like structures (Figure 3f), no other phases or textures can be found after tempering the hydrogel samples. In the course of further heating and cooling, the parallel structures frequently appear at the same location and with the same orientation. Figure 4 shows an initial stage of formation of such aggregates while cooling a diluted sample of OHD of 2 wt %. At such low concentrations, no focal conic textures can be found. This is also conclusive since the layer structuring of amphiphiles usually requires higher concentrations. Also, the clearing temperatures of gels with different concentrations have been examined. Those are the temperatures at which the transition between the mesophase with the highest temperature range and the isotropic phase occurs. The gel solution phase transition temperatures were determined by the disappearance of birefringence between crossed polars, indicating the isotropization of the samples. Afterward, cooling of the samples led to the restructuring of the hydrogel. Table 1 summarizes the results of these experiments. Both temperatures increased with the concentration of the hydrogels.

X-ray Studies. Wide-angle X-ray diffraction is another important method for the elucidation of structural features of gels. Among the most valuable information is the long *d*-spacing, which corresponds to the longest repeat distance in the supramolecular assemblies and distinguishing between different packing types such as lamellar from hexagonal. By correlating these data with molecular dimensions, as can be gained by molecular dynamics calculations, it is possible to propose models for the packing of the molecules.[35]

Figure 5a shows the X-ray diffraction pattern of a xerogel obtained at room temperature. The first-order small angle reflection clearly indicates the smectic ordering of the sample. As calculated from the diffraction pattern, the layer spacing is about 40 Å in a xerogel derived from a hydrogel with 6 wt % OHD (Figure 5b).

As can be seen in Figure 6, the maxima of the diffraction angles rise for xerogels obtained from hydrogels with higher concentrations. This finding indicates that the layer spacing decreases slightly with higher concentrations, demonstrating that the average separation between the aggregates is also affected by the water content of the original hydrogel. However, after calculating the *d*-spacing from the experimental data, at most,

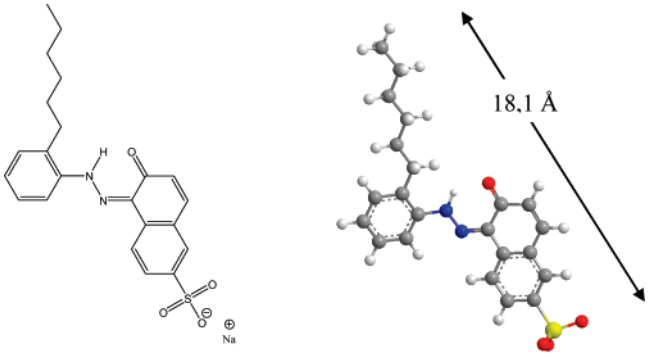

Figure 7. Structure of OHD in its tautomeric form as hydrazone optimized with the CAChe program. The longest diameter as indicated by the arrow is 18.1 Å.

TABLE 2: Smectic Layer Spacing for Xerogels Obtained by Freeze-Drying of Hydrogels with Different Concentrations

concn of original hydrogel (wt %)	*d* (Å)
4	40.9 ± 0.5
6	39.0 ± 0.5
8	38.9 ± 0.5
10	38.9 ± 0,5

only moderate changes in the *d*-values if any can be suggested within the error margin (Table 2).

MO Calculations. To correlate the information of the X-ray examination with the structure of the hydrogelator OHD, semiempirical calculations were carried out by the CAChe program. Since the exact structure of the aggregates of OHD in the gel state is unknown and many different conformations can be assumed, the calculation and construction of a structural model are very difficult and have to be speculative. On the basis of special features of the molecular structure, we made the following assumptions: the dye exists in its ionic form, and the cation makes no contribution to its cross-section dimension. Further, the calculations are based on the hydrazone form since it is known that such dyes exist predominantly, if not exclusively, in the hydrazone form and not as an azo tautomer.[36,37]

The conformation was first optimized using augmented MM3 parameters. The ground state structure of the system was then refined by performing an optimized geometry calculation in water with MOPAC using PM3 parameters. Using these assumptions, a structural model as shown in Figure 7 was derived. The length of the molecule was calculated to be 18.1 Å, which is about half of the *d*-spacing in the smectic A phase (SmA) that was derived from the X-ray analysis.

NMR Experiments. To possibly obtain more information about the aggregation mechanism on the molecular level, examinations were performed by means of ^{1}H NMR spectroscopy.

In particular, Hamada et al. have applied NMR studies extensively for the examination of various azo dyes.[38−40] But, their investigations were performed exclusively with partially fluorinated compounds utilizing ^{19}F NMR spectroscopy. Thereby, the assignment of peaks is less complicated since they appear in a well-defined and characteristic frequency range; also, signal broadening and the change in chemical shifts is of minor concern. On the other hand, the changes in the shape and shifts of the signals of protons can provide valuable information about the types of interactions between the molecules and about the functional groups involved in the aggregation process.

Therefore, we prepared a gel with 6 wt % OHD in D_2O. This gel was investigated by ^{1}H NMR experiments at different temperatures. Below 35 °C, the sample was in its gel state, and

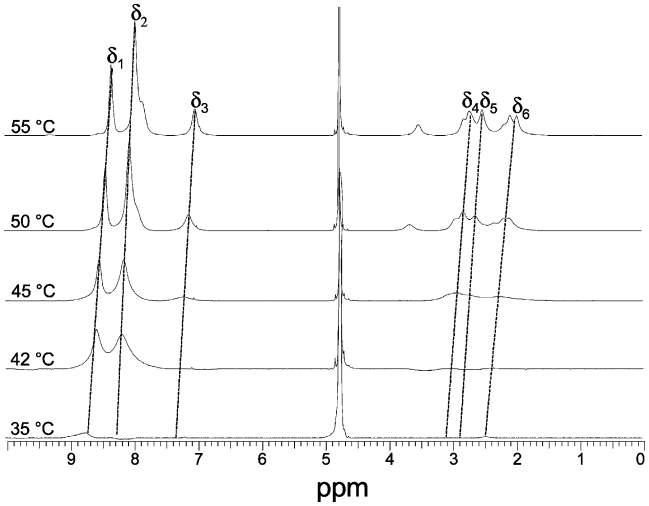

Figure 8. ^{1}H NMR spectra of the gel of OHD in D_2O at various temperatures.

TABLE 3: Temperature Shifts of Diverse Signals (ppm) of a Gel of OHD in D_2O

T (°C)	δ_1	δ_2	δ_3	δ_4	δ_5	δ_6
42	8.58	8.17	7.25	3.11	2.97	2.35
45	8.53	8.14	7.21	2.92	2.74	2.24
50	8.42	8.04	7.11	2.8	2.61	2.12
55	8.33	7.96	7.01	2.7	2.51	2.02
Dd	0.25	0.21	0.24	0.41	0.46	0.33

hardly any signals could be observed. After raising the temperature to 42 °C, two broad signals appeared in the aromatic region, marking the beginning of the gel-to-sol transition and the formation of an isotropic solution. Upon further heating, the intensity of these signals increased, and additional signals appeared in the aromatic region (Figure 8).

On a molecular level, the disaggregation of the supramolecular arrangement of the dye molecules led to the shielding of the aromatic protons, which then appeared in the spectra. This finding can be attributed to hydrophobic arene−arene stacking interactions in the aggregated sample of OHD.[41,9] Along with the new aromatic signals, those of the aliphatic protons of the hexyl substituent begin to appear between 2 and 4 ppm, indicating their participation in the intermolecular binding as well. This is presumably due to van der Waals forces and hydrophobic interactions of the side chain.[42] Because of the simultaneous occurrence of both stacking and hydrogen bonding, the signals become rather broad.[41] Furthermore, all signals of OHD were gradually shifted upfield upon heating. Table 3 provides an overview of the changes in the chemical shifts of certain easily observable signals (note that the signals for the aliphatic protons δ_4, δ_5, and δ_6 at 35 and 42 °C could only be seen after magnification and are not present in the spectra shown in Figure 8).

Other than in DMSO, a precise assignment of the various peaks is complicated, and only a clear distinction between aromatic and non-aromatic peaks can be made. However, in the aliphatic region, the signal with the lowest value can be assigned to the protons of the methyl end-group of the hexyl side chain. This signal exhibits the smallest shift in the course of raising the temperature, and therefore, its contribution to the hydrophobic binding ought to be weaker than that of its neighboring protons. This implies that the hexyl groups are not located between the aromatic systems but aim outward of this stacking. In this arrangement, the chemical shifts of the inner protons can be expected to change more markedly with

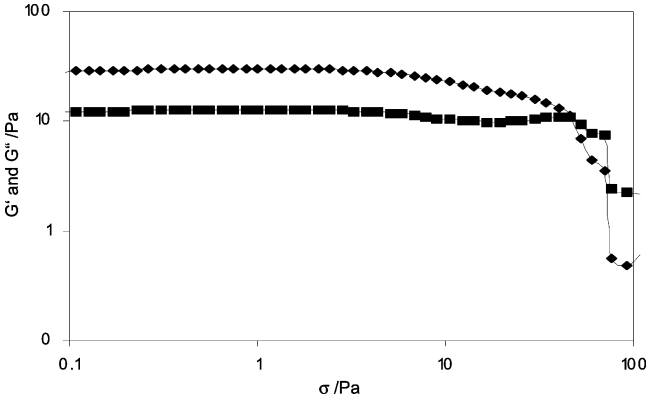

Figure 9. Rheological plot of a typical amplitude sweep experiment (storage modulus G' (◆) and viscous modulus G'' (■) vs shear stress σ).

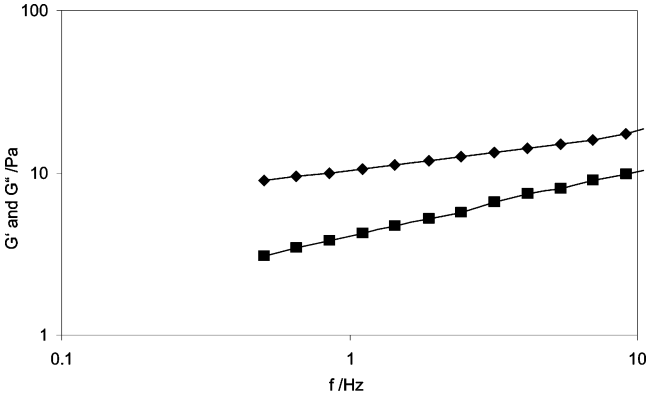

Figure 10. Dynamic moduli (storage modulus G' (◆) and loss modulus G'' (■)) as a function of the oscillatory frequency for a hydrogel of OHD of 6 wt % at 25 °C. The strain of 0.1 Pa applied in this experiment is within the linear viscoelastic region as determined with amplitude sweep experiments.

disaggregation since they are located closer to the centers of the adjacent rings.[43] The upfield shifts of the aromatic protons reflect the close approach of the aromatic rings in the stacking interaction.[44] Moreover, this indicates that the most favored orientation of adjacent molecules in the stack is one in which the aromatic units possess a parallel configuration.[45]

In summary, it can be concluded from the NMR experiments that the main driving forces for the self-assembly of the gelator molecules are aromatic stacking and van der Waals interactions, leading to a parallel arrangement in the supramolecular aggregates of OHD.

Rheological Experiments. Rheological experiments are a valuable amendment to the previous structural analysis since they provide information about the dynamic mechanical properties of the sol−gel process.[46] They enable the distinction between fast and slow hydrogelators as well as strong and weak gels and thus offer also a convenient method to evaluate the potential for practical applications due to the strength and flexibility of a given gel.[47]

The information of amplitude sweep experiments is usually used to optimize the settings for further rheological experiments where periodic stress has to be applied within the appropriate amplitude range defining the linear regime. A sample of a hydrogel of OHD was subjected to an increasing oscillation stress σ in an amplitude sweep experiment. Both dynamic moduli show linear responses between 0.1 and 6 Pa, pointing out that the sample's structure is maintained at such a low shear stress (Figure 9).

The storage modulus G' decreases slowly between 6 and 45 Pa. Apparently, the applied vibrations already cause the breaking of the structure. Finally, the yield stress is reached between 45 and 60 Pa, and the gel breaks since its intermolecular forces have been overcome. Both the storage modulus G' and the viscous modulus G'' drop abruptly. The resulting system shows the rheological properties typical of a liquid rather than that of a solid.

In the frequency sweep experiment, the hydrogel exhibits typical characteristics of a soft solid.[48] The storage modulus G' is larger than the loss modulus G'' at all frequencies. However, G' is only about 2-fold higher than G'', which indicates that a dissipation of energy through viscous mechanisms is dominant and that slow rearrangements take place in the gel. This is further supported by the significantly sloped G' versus frequency f, which points to a limited tolerance of the hydrogel to external forces (Figure 10).

The duration and speed of gel formation has been followed by time sweep experiments.[49] For that purpose, a warmed solution of OHD at a concentration of 6 wt % was introduced between the plates of the rheometer. After the temperature fell below the sol-to-gel transition temperature of about 54 °C, there was a sharp increase in the storage modulus G' at a characteristic time of the aggregation process (Figure 11). The gel then formed very quickly, leading to a viscoelastic system within less than 5 min. This shows that OHD is a remarkably fast hydrogelator, even more when considering that the shearing action inherently retards the structure growth. In many cases, it takes hours for the gelation process to complete even without shearing,[48,50−52] and not many examples for comparably quick hydrogelators are known.[53−55]

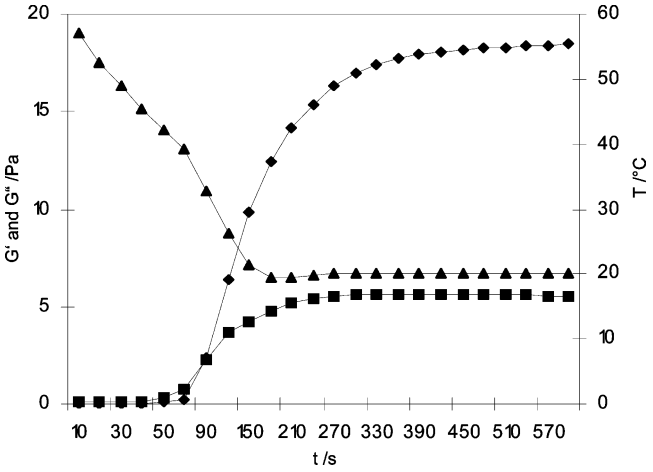

Figure 11. In the time sweep experiment, changes of G' (◆) and G'' (■) were measured with temperature (▲) and time.

Values for gel-to-sol transition temperatures (T_{GS}) are collected while heating a gel until flow occurs. The sol-to-gel transition temperatures (T_{SG}) are the temperatures where a viscoelastic gel is formed from a solution of a gelator during cooling. The crossover point of the two dynamic moduli indicates when the sample has reached a transition temperature. Usually, it is found that the values for the two transition temperatures T_{GS} and T_{SG} differ due to hysteresis. Such is also the case with our hydrogelator. When gels of OHD are slowly heated, there is a crossover point of the elastic and viscous moduli at 52 °C. This is the T_{GS} where the gel begins to flow and becomes a liquid solution. During cooling, the moduli begin to increase below 50 °C until they exhibit a second crossover point at about 43 °C, where the gel is newly formed and the sample becomes predominantly viscoelastic. During the tem-

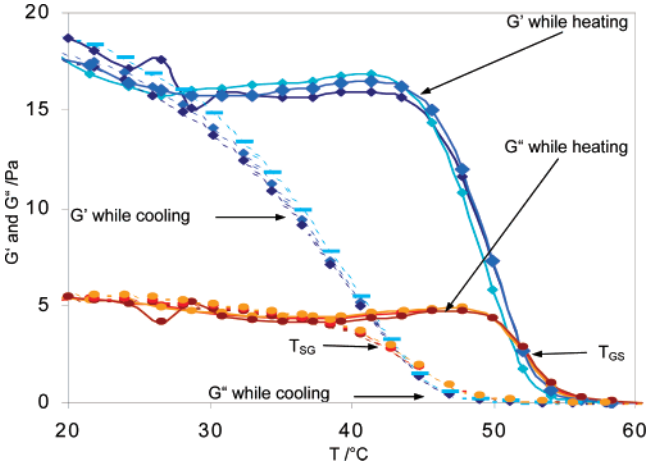

Figure 12. Overlap of the diagrams of three successive temperature sweep experiments for a hydrogel of 6 wt % at a frequency of 0.1 Hz and amplitude of 2%. The blue lines show the changes of the storage modulus G' as a function of temperature, while the red lines represent the values determined for G''. The dotted lines show the changes of the dynamic moduli during cooling, whereas the data for the normal lines were collected during heating of the sample.

perature sweep experiments, we performed three cycles of heating and cooling of the same sample between 20 and 60 °C. Figure 12 shows an overlap of the collected data. As can be seen, the curves are almost congruent. This proves to be an excellent reversibility of the gel formation. Furthermore, the transitions take place at mild gelation conditions. Both are highly sought after properties for various applications.

Model for the Hierarchical Self-Assembly of OHD. Combining the structural information gathered by the various analytical techniques, the following model of the hierarchical self-assembly of OHD is proposed. As deduced from NMR experiments, the molecules exhibit a coplanar stacking. The intermolecular distance of 5 Å was calculated from the small angle X-ray reflexes. Besides $-\pi-\pi$ stacking, hydrogen bonds should be the main driving force for this aggregation. Both interactions possess a precise directing ability, leading to a well-ordered orientation.

The amphiphilic nature of the molecules then causes the formation of a secondary structure. OHD possesses a negatively charged and hydrophilic sulfonate unit attached to a hydrophobic residue. Within this residue, aromatic moieties form a rigid core bearing the rather flexible hexyl chain at the end (Figure 13 a). In polar environments such as water, hydrophobic forces lead to arrangements of the molecules, which minimize the repulsive forces between the hydrophobic regions and the solvent and maximize attractive forces due to hydrogen bonding and ionic interactions between the solvent molecules and the hydrophilic parts of the amphiphile. In our case, this can be achieved by a tail-to-tail arrangement of the molecules, leading to structures with the alkyl chain in the inside and the polar sulfonate group pointing outward (Figure 13b). The calculated fully extended molecular length of OHD is 18.1 Å, which corresponds to a little less than half of the *d*-spacing of 40 Å as was found by XRD. This implies an all-trans conformation of the hexyl side chain and no interdigitation between the chains of adjacent molecules. There remains a difference of about 4 Å between the double length of OHD and the value for the *d*-spacing. However, the diameter of OHD has been calculated omitting the sodium counterion. This and the entrapped water molecules can account for the difference. On this basis, several models based on the formation of aggregates with tail-to-tail ordering of OHD can be proposed. Among them are various micellar

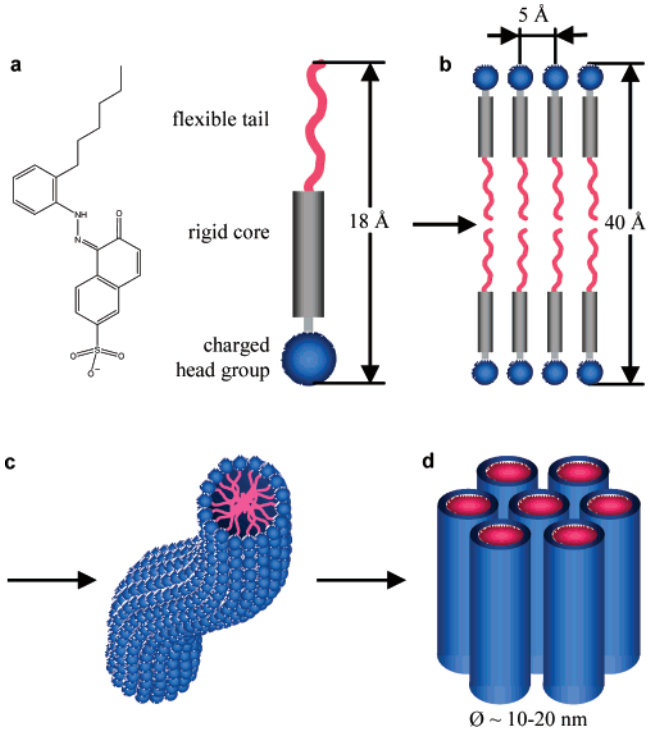

Figure 13. (a) Schematic structure of OHD. (b) Tail-to-tail arrangement of molecules of OHD. (c) Rod-shaped micelle. (d) Hexagonal array made out of rods.

packing structures as well as layer structures and morphologies as fibers and sheets as are frequently found for amphiphiles. The obtained *d*-spacing corresponds well to the diameter of a micellar rod as shown in Figure 13c.

The POM studies showed that OHD forms a hexagonal phase after thermal cycling. Such a phase can be obtained by the hexagonal packing of rod-like micelles, leading to arrays with diameters in the range of 12 nm (Figure 13c,d). In our high-resolution microscopic investigations of hydrogels as well as of xerogels, we found fibers of such dimensions as shown in Figure 2b. These fibers can form the walls of the channels. A further phase identified by POM was the bilayer or lamellar phase. As previously mentioned, such phases are comparable to the smectic phases of thermotropic liquid crystals. In such systems, the molecules are arranged in a double layer with the polar groups pointing outward. Since such layers can slide easily past each other, this might be the reason why hydrogels of OHD possess a relatively low strength as was found in the rheological experiments. On the other hand, this packing facilitates rapid reorganization after disturbance and also fast formation, leading to a quickly responding system with a low gelation time. Furthermore, this might be the reason for the capability of OHD to form gels from ground powders of xerogels at room temperature. When grinding lyophilized samples, the global super-structure of the channels is destroyed. However, the resulting wall fragments should still be composed of fibers and rods ordered in parallel since these possess much smaller dimensions than the channels, and grinding only results in their partial destruction. When wetted anew, reformation of the walls proceeds easily by rapid assembly of these preordered building blocks. The rebuilding of the liquid crystalline phase thus is the main driving force that makes OHD a fast responding thermal and also instant hydrogelator.

Acknowledgment. This work was generously supported by the Deutsche Forschungsgemeinschaft (Emmy-Noether-Pro-

gram) and by the Fonds der Chemischen Industrie. The authors also express their gratitude to Prof. Friedrich and W. Schemionek for their assistance with the rheological measurements, to Prof. Finkelmann and his group for their indispensable help with POM and X-ray analyses, and to Dr. Danilewsky for his help with SEM measurements.

References and Notes

(1) Flory, P. J. *Discuss. Faraday Soc.* **1974**, *57*, 7.
(2) Lee, K. Y.; Mooney, D. J. *Chem. Rev.* **2001**, *101*, 1869.
(3) Phillips, R. J.; Deen, W. M.; Brady, J. F. *J. Colloid Interface Sci.* **1990**, *139*, 363.
(4) Kiyonaka, S.; Sugiyasu, K.; Shinkai, S.; Hamachi, I. *J. Am. Chem. Soc.* **2002**, *124*, 10954.
(5) Rees, G. D.; Robinson, B. H. *Adv. Mater.* **1993**, *5*, 608.
(6) Fuhrhop, J.-H.; Boettcher, C. *J. Am. Chem. Soc.* **1990**, *112*, 1768.
(7) Das, D.; Dasgupta, A.; Roy, S.; Mitra, R. N.; Debnath, S.; Das, P. K. *Chem.—Eur. J.* **2006**, *12*, 5068.
(8) Nakashima, T.; Kimizuka, N. *Adv. Mater.* **2002**, *14*, 1113.
(9) John, G.; Jung, J. H.; Masuda, M.; Shimizu, T. *Langmuir* **2004**, *20*, 2060.
(10) Lipowitz, A. *Ann. Chem. Pharm.* **1841**, *38*, 348.
(11) Menger, F. M.; Caran, K. L. *J. Am. Chem. Soc.* **2000**, *122*, 11679.
(12) Sangeetha, N. M.; Maitra, U. *Chem. Soc. Rev.* **2005**, *34*, 821.
(13) Maitra, U.; Mukhopadhyay, S.; Sarkar, A.; Rao, P.; Indi, S. S. *Angew. Chem., Int. Ed.* **2001**, *40*, 2281.
(14) Lehn, J.-M. *Rep. Prog. Phys.* **2004**, *67*, 249.
(15) Hartgerink, J. D.; Beniash, E.; Stupp, S. I. *Science (Washington, DC, U.S.)* **2001**, *294*, 1684.
(16) Uhrich, K. E.; Cannizzaro, S. M.; Langer, R. S.; Shakesheff, K. M. *Chem. Rev.* **1999**, *99*, 3181.
(17) Tiller, J. C. *Angew. Chem., Int. Ed.* **2003**, *42*, 3072.
(18) Xing, B. G.; Yu, C. W.; Chow, K. H.; Ho, P. L.; Fu, D. G.; Xu, B. *J. Am. Chem. Soc.* **2002**, *124*, 14846.
(19) Bieser, A. M.; Tiller, J. C. *Chem. Commun.* **2005**, 3942.
(20) Takahashi, A.; Sakai, M.; Kato, T. *Polym. J.* **1980**, *12*, 335.
(21) Bhattacharya, S.; Ghanashyam Acharya, S. N. *Langmuir* **2000**, *16*, 87.
(22) Vauthey, S.; Santoso, S.; Gong, H.; Watson, N.; Zhang, S. *Proc. Natl. Acad. Sci. U.S.A.* **2002**, *99*, 5355.
(23) Kogiso, M.; Ohnishi, S.; Yase, K.; Masuda, M.; Shimizu, T. *Langmuir* **1998**, *14*, 4978.
(24) Pang, S. F.; Zhu, D. B. *Chem. Phys. Lett.* **2002**, *358*, 479.
(25) Simmons, B. A.; Irvin, G. C.; Agarwal, V.; Bose, A.; John, V. T.; McPherson, G. L.; Balsara, N. P. *Langmuir* **2002**, *18*, 624.
(26) Nakazawa, I.; Masuda, M.; Okada, Y.; Hanada, T.; Yase, K.; Asai, M.; Shimizu, T. *Langmuir* **1999**, *15*, 4757.
(27) Holmes, M. C.; Charvolin, J. *J. Phys. Chem.* **1984**, *88*, 810.
(28) Hartshorne, N. H. *The Microscopy of Liquid Crystals*; Microscope Publications Ltd.: London, 1974.
(29) Gray, G. W. *Liquid Crystal and Plastic Crystals*; Ellis Horwood Ltd.: New York, 1974; Vols. 1 and 2.
(30) Demus, D.; Richter, L. *Textures of Liquid Crystals*; Verlag Chemie: Weinheim, Germany, 1978.
(31) Ujiie, S.; Uchino, H.; Iimura, K. *Chem. Lett.* **1995**, 195.
(32) Lai, L. L.; Su, F. Y.; Hung, C. H. *Liq. Cryst.* **2004**, *31*, 773.
(33) Lai, L. L.; Lin, H. C. *Liq. Cryst.* **2000**, *27*, 707.
(34) Mamiya, J.; Kanie, K.; Hiyama, T.; Ikeda, T.; Kato, T. *Chem. Commun.* **2002**, 1870.
(35) Estroff, L. A.; Leiserowitz, L.; Addadi, L.; Weiner, S.; Hamilton, A. D. *Adv. Mater.* **2003**, *15*, 38.
(36) Gordon, P. F. *Organic Chemistry in Color*; Gregory, P., Ed.; Springer: Heidelberg, 1983; Vol. XI.
(37) Hamada, K.; Yamada, K.; Mitsuishi, M.; Ohira, M.; Mesuda, K. *J. Chem. Soc., Faraday Trans.* **1995**, *91*, 1601.
(38) Hamada, K.; Yamada, K.; Mitsuishi, M.; Ohira, M.; Miyazaki, K. *J. Chem. Soc., Chem. Commun.* **1992**, 544.
(39) Hamada, K.; Take, S.; Iijima, T.; Amiya, S. *J. Chem. Soc., Faraday Trans. 1* **1986**, *82*, 3141.
(40) Hamada, K.; Hirano, T.; Yamada, K.; Mitsuishi, M. *Dyes Pigm.* **1993**, *22*, 151.
(41) Brunsveld, L.; Vekemans, J.; Hirschberg, J.; Sijbesma, R. P.; Meijer, E. W. *Proc. Natl. Acad. Sci. U.S.A.* **2002**, *99*, 4977.
(42) Snip, E.; Shinkai, S.; Reinhoudt, D. N. *Tetrahedron Lett.* **2001**, *42*, 2153.
(43) Vogtle, F.; Weber, E. *Angew. Chem., Int. Ed.* **1979**, *18*, 753.
(44) Goswami, S.; Hamilton, A. D.; Vanengen, D. *J. Am. Chem. Soc.* **1989**, *111*, 3425.
(45) Hamada, K.; Kubota, H.; Ichimura, A.; Iijima, T.; Amiya, S. *Ber. Bunsen-Ges. Phys. Chem.* **1985**, *89*, 859.
(46) Almdal, K.; Dyre, J.; Hvidt, S.; Kramer, O. *Makromol. Chem., Macromol. Symp.* **1993**, *76*, 49.
(47) Ferry, J. D. *Viscoelastic Properties of Polymers*; Wiley: New York, 1980.
(48) Yao, S.; Beginn, U.; Gress, T.; Lysetska, M.; Wurthner, F. *J. Am. Chem. Soc.* **2004**, *126*, 8336.
(49) Terech, P.; Bouaslaurent, H.; Desvergne, J. P. *J. Colloid Interface Sci.* **1995**, *174*, 258.
(50) Kiyonaka, S.; Sada, K.; Yoshimura, I.; Shinkai, S.; Kato, N.; Hamachi, I. *Nat. Mater.* **2004**, *3*, 58.
(51) Suzuki, M.; Yumoto, M.; Kimura, M.; Shirai, H.; Hanabusa, K. *New J. Chem.* **2002**, *26*, 817.
(52) Chujo, Y.; Yoshifuji, Y.; Sada, K.; Saegusa, T. *Macromolecules* **1989**, *22*, 1074.
(53) Yang, Z. M.; Gu, H. W.; Zhang, Y.; Wang, L.; Xu, B. *Chem. Commun.* **2004**, 208.
(54) Bhattacharya, S.; Acharya, S. N. G. *Chem. Mater.* **1999**, *11*, 3504.
(55) Nowak, A. P.; Breedveld, V.; Pakstis, L.; Ozbas, B.; Pine, D. J.; Pochan, D.; Deming, T. J. *Nature (London, U.K.)* **2002**, *417*, 424.